scientific reports

Check for updates

OPEN

Automated characterization of the gray matter white matter distribution demonstrates age-related decline

Joan Y. Song[1], Roman Fleysher[2], Kenny Ye[3], Mimi Kim[3], Jenasis Ortega[1], Molly E. Zimmerman[4], Richard B. Lipton[5] & Michael L. Lipton[6,7]✉

Neuroimaging techniques offer valuable insights into the structural characteristics of the brain. For example, a salient feature of the cerebrum is the distinct transition of voxel intensity at the interface of gray matter (GM) and white matter (WM). Leveraging the inherent difference in tissue composition – lower GM and higher WM signal on T1-weighted (T1W) magnetic resonance imaging (MRI) – we introduce a novel metric, distance between peaks of WM and GM intensities, which unlike GM/WM contrast does not rely on segmentation and demonstrate its efficacy in capturing age-related effects. A single 3D T1W whole brain MRI (MP-RAGE, 1 mm isotropic voxels) image was acquired at 3 Tesla from each of 178 healthy participants (18–91 years (54.78 ± 21.37), 103 Female) between 2019 and 2023. Before peak differentiation calculation, non-brain tissue was removed, and voxel intensities were corrected for RF coil profile. We define peak differentiation as the difference between means of two Gaussians fitted to the T1W voxel intensities, scaled by their common standard deviation. Age dependence of peak differentiation is examined using a linear model with biological sex included as a covariate. Similar analysis was performed by limiting to voxels within 5 mm of the Freesurfer-defined cerebral gray matter-white matter interface (GWI) in six lobes: orbitofrontal, frontal, occipital, temporal, parietal, and cingulate. Reduced whole-brain peak differentiation was associated with older age (β_1 = − 0.012, 95% CI [-0.0132, -0.0105], $p < 0.001$), indicating a decline in WM-GM distribution sharpness with advancing age. Each GWI subregional peak differentiation exhibited the same pattern of decline with age, but differed in magnitude region ($p < 0.001$). The cingulate region exhibited the sharpest decline with age (β_1 = -0.014, 95% CI [− 0.0160, − 0.0126], $p < 0.001$). We demonstrate feasibility of an automated whole brain peak differentiation measurement to characterize brain aging in a group of healthy individuals, with minimal reliance on segmentation or other processing, with implications for understanding normal trajectories and identifying pathological deviations from expected aging processes.

Tissue composition of brain white matter (WM) and gray matter (GM) differ. WM is predominantly comprised of parallel bundles of myelinated axons, whereas GM exhibits a much greater proportion of structures such as cell bodies and dendrites. Due to differences in their magnetic properties, a sharp distinction in voxel intensity can be appreciated at the gray matter-white matter interface (GWI) on T1-weighted images (T1W) acquired using magnetic resonance imaging (MRI). The imaging features mirror the appearance of the GWI on gross anatomy. Quantification of this imaging feature, especially on widely available T1W image, could facilitate assessment of brain health and detection of pathological processes at the GWI.

The GWI is a site of pathology in many brain disorders, including traumatic brain injury[1–3], focal cortical dysplasia[4], Zika virus infection[5], progressive multifocal leukoencephalopathy[6], multiple sclerosis[7] and Alzheimer's disease[8]. Prior neuroimaging studies of these disorders have largely reported qualitative features

[1]Dominick P Purpura Department of Neuroscience, Albert Einstein College of Medicine, Bronx, NY, USA. [2]Department of Radiology, Columbia University Irving Medical Center, New York, NY, USA. [3]Department of Epidemiology and Population Health, Albert Einstein College of Medicine, Bronx, NY, USA. [4]Department of Psychology, Fordham University, Bronx, NY, USA. [5]Saul R. Korey Department of Neurology, Albert Einstein College of Medicine and Montefiore Medical Center, Bronx, NY, USA. [6]Department of Biomedical Engineering, Columbia University, New York, NY, USA. [7]Present address: Department of Radiology, Columbia University Irving Medical Center, 530 W 166th St., New York, NY, USA. ✉email: mll2219@cumc.columbia.edu

of the GWI[2,4–6]. Normal aging also alters the GWI, with prior studies reporting age-related changes in tissue contrast at this location on T1W MRI[9]. To quantify the GWI tissue transition by computing tissue contrast, for example, studies have segmented GM and WM to selectively extract voxel intensity from each tissue class, for example at 35% thickness of cortical GM and 1 mm into WM[9]. This approach requires preprocessing to accurately sample GM and WM voxel intensities and could be impacted by segmentation errors. Furthermore, cortical thickness itself is known to decrease with age and may conflict with cortical GM intensity sampling. Furthermore, there can be utility in characterizing GM-WM distribution instead of intensity contrast.

In this study, we propose an approach which takes the unsegmented brain as an input and measures the separation between the distributions of WM and GM voxel intensities as an index of tissue contrast around the GWI. We illustrate the method by detecting expected age-related decline in tissue differentiation on T1W images around the GWI. In addition to existing analysis techniques such as region of interest voxel intensity and GM/WM contrast, this method could be used to identify loss of normally sharp tissue distinction around the GWI in the setting of disease.

Methods

Study cohort

This analysis includes data from a total of 178 healthy participants, spanning 18 to 91 years of age (54.78 ± 21.37) of which 103 are females, enrolled in two normative lifespan cohorts at Albert Einstein College of Medicine from 2019 to 2023, 76 participants from the Einstein Aging Study (EAS)[10] and 102 from the Einstein Lifespan Study (Lifespan)[11]. Both studies were approved by the institutional review board of Albert Einstein College of Medicine, obtained written informed consent from each participant, and complied with HIPAA. All methods were performed in accordance with the relevant guidelines and regulations. Inclusion criteria for the EAS included residence in the greater New York City area, English fluency, age of 70 or older. EAS exclusion criteria included dementia, visual or auditory impairments that would preclude neuropsychological testing, active psychiatric symptomatology that would interfere with the ability to complete assessments, contraindication to MRI and non-ambulatory status. Lifespan inclusion criteria included residence in the greater New York City area, English fluency, and age 18–65 years. Lifespan exclusion criteria included history of head injury, diagnosed psychiatric disorder (Bipolar Disorder, Schizophrenia, Generalized Anxiety Disorder, Major Depression, Substance Use Disorder), neurological disorder other than headache, diabetes, hypertension, heart disease, stroke, contraindication to MRI or recreational drug use within previous thirty days.

Image acquisition and processing

All data were collected on the same 3.0T Philips Achieva TX scanner using a 32-channel head coil (Philips Medical Systems, Best, The Netherlands). 3D T1 weighted magnetization-prepared rapid acquisition gradient echo (MPRAGE) imaging was performed with TR/TE/TI = 9.9/4.6/900ms, α = 8°, SENSE factor along SI/RL = 2/2.6, 1 mm isotropic resolution, 240 × 188 × 220 matrix. MPRAGE train length = 154 along z-phase encode, time between inversions = 2375msec, bandwidth = 145.1 Hz/mm, and scanner's built-in receive profile uniformity correction. An auxiliary field map scan was acquired using FOV = 250 mm, 3 mm isotropic resolution, TR = 26ms, TE/ΔTE = 2.5/2.3ms, α = 26° and SENSE factor = 2 (anterior-posterior) x 2 (head-foot). The field map is used to correct small susceptibility-induced distortions in T1-weighted scans[12,13]. The relative separation between GM and WM tissue peaks remains stable across physiologically relevant TI values (Supplemental Fig. 1). Non-brain tissue was removed using SynthStrip[14]; in addition to the receive coil profile correction inherent to 3.0T Philips Achieva TX scanner, which involves image reconstruction based on in situ coil calibration, correction for RF coil profile was calculated using FMRIB's Automated Segmentation Tool (FAST)[15,16]. All images underwent structured assessment for image quality, motion artifacts and quality of brain extraction, performed by experienced, trained raters.

Peak differentiation calculation

Whole-brain T1-weighted voxel intensities (Fig. 1 (a)) were linearly scaled to a range of 0 to 3000. The histogram exhibits two peaks, corresponding to intensities of voxels in gray and white matter (Fig. 2).

To quantify distance between these two peaks, all voxels with scaled intensities between 400 and 2800 were fit to a mixture of two gaussian distributions of equal variance. The Gaussian distribution is an excellent approximation to Rician distribution for signal-to-noise ratios (SNR) above 5, which is definitely fulfilled for gray and white matter signals[17]. To stabilize fitting, the 400–2800 scaled intensity window was selected empirically based on visual inspection of the intensity distributions to exclude extreme histogram tails while preserving the GM and WM peaks. The lower cutoff largely excludes CSF voxels, while the upper cutoff removes the small number of high–intensity vascular voxels. Importantly, modest adjustments to these window limits are not expected to alter the peak differentiation metric.

Peak differentiation is defined as the difference in means (μ_1, μ_2) of the two fitted Gaussian distributions, scaled by their common standard deviation (σ) as shown in Eq. 1:

$$peak\ differentiation = \frac{\mu_2 - \mu_1}{\sigma} \quad (1)$$

Maximum likelihood estimates of these parameters were obtained using the 'mclust' package in R[18].

For each participant, whole-brain peak differentiation using all brain voxels (Fig. 1 (a)) was calculated. A graphical representation of the peak differentiation method is shown in Fig. 2.

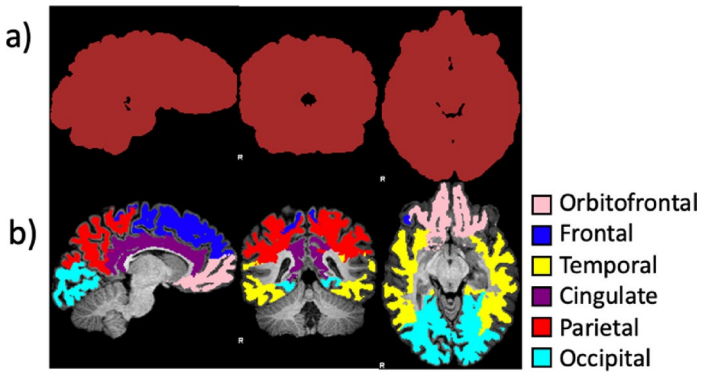

Fig. 1. (**a**) Whole brain segmentation includes all voxels. (**b**) Lobar segmentation includes voxels in white and gray matter within 5 mm from the Freesurfer defined GWI.

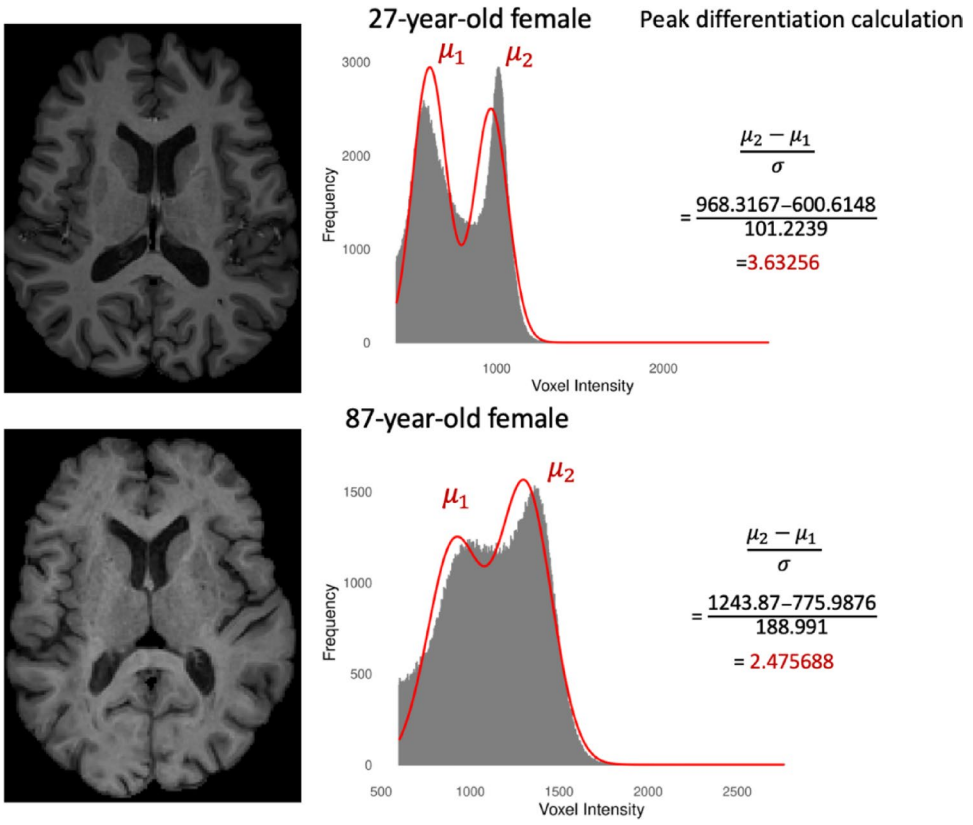

Fig. 2. Sample peak differentiation calculations. Whole brain voxel intensity histograms from a 27-year-old female and an 87-year-old female. Peak differentiation calculations are shown.

Association of peak differentiation with age

We fit the following linear model to the whole brain peak differentiation as a function of age and other covariates:

$$Y_i = \beta_0 + \beta_1 Age_i + \beta_2 Sex_i + e_i \quad (2)$$

In Eq. 2, Y_i denotes the whole brain peak differentiation for participant *i;* β_0 is an intercept term; Age_i is the i^{th} subject's age at which imaging was collected; coefficient β_1 denotes the independent cross-sectional association of age with the peak differentiation. Biological sex was included as covariate Sex_i; coefficient β_2 denotes the association of biological sex (male compared to female) with peak differentiation and e_i is a random error term. Analyses were performed in R[19].

Subregional peak differentiation

To investigate regional differences, we segmented brain into orbitofrontal, frontal, occipital, temporal, parietal, and cingulate subregions defined to be within 5 mm of the Freesurfer 7-defined cerebral GWI[20] (Fig. 1 (b)). Voxels were sorted into regions by their shortest Euclidean distance orthogonal to the plane of the GWI interface which was also segmented into the aforementioned regions. Peak differentiation was then computed using voxels within each of these six subregions (Eq. 1).

To test if the peak differentiation association with age varies across the six brain regions, we compared two linear mixed effects models using likelihood ratio tests using R library lme4. One model (Eq. 3) assumes the same effect of age across the different regions; the other model (Eq. 4) allows different effects of age for each region.

$$Y_{iR} = \beta_{i0} + \alpha_R + \beta_1 Age_i + \beta_2 Sex_i + e_{iR} \quad (3)$$

$$Y_{iR} = \beta_{i0} + \alpha_R + \beta_{1R} Age_i + \beta_2 Sex_i + e_{iR} \quad (4)$$

In Eqs. 3 and 4, β_{i0} represents the random subject effect for participant *i*; Y_{iR} denotes the regional peak differentiation for participant *i* in region *R*; α_R denotes the region-specific intercept offset (e.g. "parietal"), $\sum \alpha_R = 0$. β_1 in (Eq. 3) is the common age effect in that model, and β_{1R} in (Eq. 4) represents the region-specific age effect.

Measure validation

To evaluate whether our peak differentiation measure is robust to the noise of the images, we compared the whole brain peak differentiation on paired low and high noise images on the same participants at the same visits. For each of two participants from whom we acquired 6 repeated T1W scans at a single visit, a low noise image was generated by averaging the six T1W scans. The images of one scan are of high noise. Since the noise level of the high noise images should be square root of 6≈2.45 times that of the noise in low noise images. If σ in Eq. 1 was dominated by noise of the image, we expect peak differentiation of the low noise images to be similarly greater than those of corresponding high noise images.

Furthermore, to verify that the observed association between peak-differentiation and age is not driven primarily by σ, we tested the association between σ, μ1, μ2 and μ2 − μ1 and age using a linear regression model, with biological sex as a covariate.

It is possible to perform the peak differentiation calculation without FAST RF coil profile correction and we include the calculations and age association analyses to further validate the robustness of this measure.

We also calculated intracranial volume (ICV) using Freesurfer 7[20] and included it as a covariate.

Results

Lower peak differentiation over the whole brain is significantly associated with older age (β_1 = -0.012, 95% CI [-0.0132, -0.0105], $p < 0.001$) (Fig. 3; Table 1). Peak differentiation for each GWI subregion shows the same pattern of decline with age (Fig. 4; Table 1), but the declines differ by region ($p < 0.001$). Therefore, we report statistical findings from Eq. 4, with the cingulate region exhibiting the sharpest decline with age (β_1 = -0.0143, 95% CI [−0.0160, −0.0126]; Table 1). We found no statistically significant effect of biological sex on peak differentiation for whole brain or for any of the six GWI subregions (Table 1).

For each of two participants that had repeated T1W images at a single visit, the whole-brain peak differentiation of the low noise and high noise images were nearly identical, with a ratio at 1.01 and 1.004 respectively, suggesting that our peak-differentiation measure is robust to the noise level of the images. The signal to noise ratio in the white matter of individual high-noise images is about 40.

Unlike peak differentiation association with age, the directionality of standard deviation association with age is different in different regions (Supplemental Table 1). Whole-brain, orbitofrontal region, occipital region, and temporal region standard deviation associations were positively associated with age; frontal and cingulate regions have negative associations with age. Parietal region standard deviations were not associated with age (Supplemental Table 1). μ2 − μ1 is inversely associated with age in all regions but not in the whole brain measure (Supplemental Table 2). σ, μ1, and μ2 are associated with age in some regions but not others (Supplemental 1–4).

We show similar peak differentiation associations with age in the whole brain and GWI subregions when we used non- bias field corrected images to calculated peak differentiation (Supplemental Table 5). We show that age dependence of peak differentiation remains significant with ICV included as a covariate and ICV, as a covariate, is not significantly associated with peak differentiation (Supplemental Table 6).

Discussion

Peak differentiation recapitulates expected T1W aging associations in a health cohort

Contrast between GM and WM tissues on T1W of a young healthy brain is visually sharp but becomes less distinct at older age. Decline of peak differentiation at older age reflects this merging of the GM and WM pixel intensities. The linear correlation between age and peak differentiation we identified across a wide age range demonstrates a consistent aging effect in healthy individuals from at least the third decade. This finding points to aging as an ongoing process across adulthood; whole brain peak differentiation is expected to decrease by 0.12 ± 0.0067 with one decade of aging. Prior studies have reported age-related lower WM volume[21], GM volume[22], and cortical thickness[23] on T1W imaging. Our results are consistent with prior qualitative[24] and quantitative[9,25–27] findings of lower GM/WM contrast in association with older age. Although conceptually distinct from absolute T1-weighted intensity, our peak-differentiation metric is consistent with prior imaging–histology correlations showing that T1-weighted hypointensities co-localize with reduced axonal density on postmortem histology[28]and

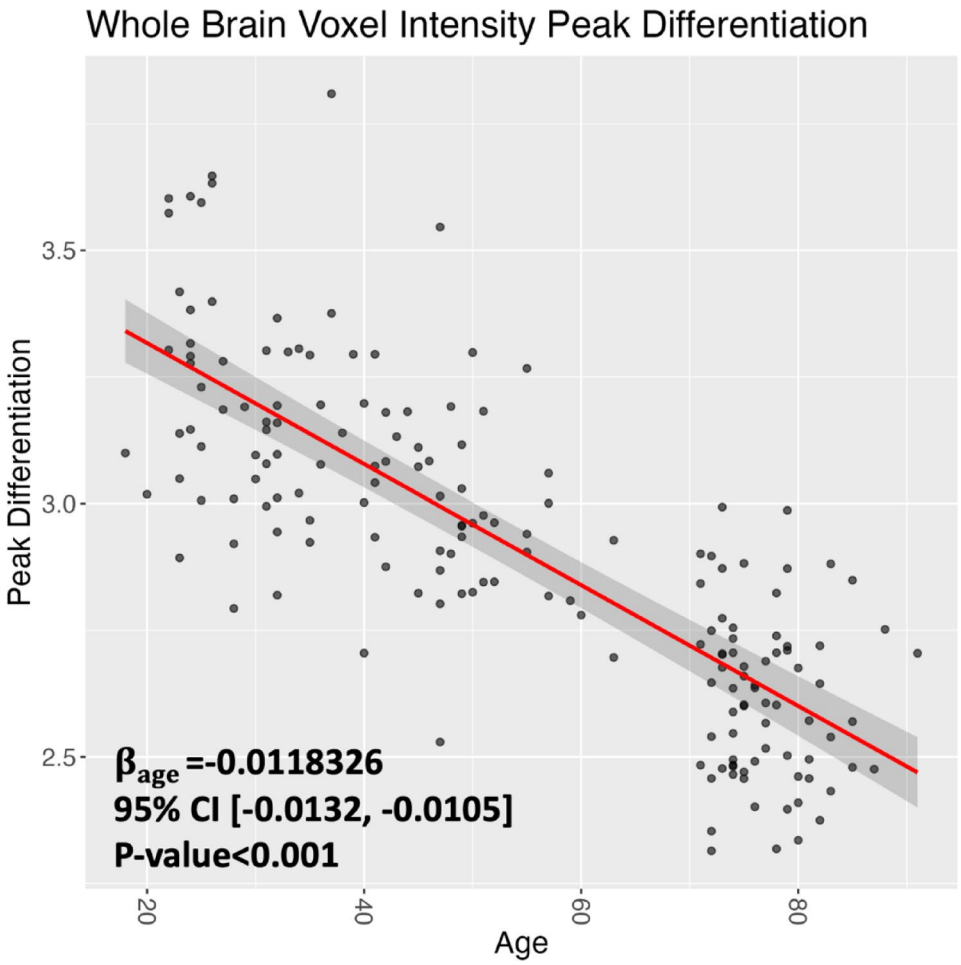

Fig. 3. Whole Brain peak differentiation associations with age ($n = 178$). Peak differentiation is plotted on y-axis. Chronological age is plotted on the x-axis. Lower peak differentiation is associated with higher age.

Region	Age		Biological sex		Adjusted R^2
	$\widehat{\beta}_1$ (per year)	P-value	$\widehat{\beta}_2$ (M vs. F)	P-value	
Whole brain	− 0.0118326	< 0.001	0.0077637	0.79	0.6394
Orbital (within 5 mm from GWI)	− 0.0127646	< 0.001	0.0060184	0.875	0.1157
Occipital (within 5 mm from GWI)	− 0.006067	< 0.001	− 0.004394	0.867	0.3611
Parietal (within 5 mm from GWI)	− 0.0126266	< 0.001	− 0.0356119	0.314	0.574
Cingulate (within 5 mm from GWI)	− 0.0143189	< 0.001	− 0.0525841	0.165	0.6019
Frontal (within 5 mm from GWI)	− 0.012727	< 0.001	0.005779	0.876	0.5591
Temporal (within 5 mm from GWI)	− 0.008980	< 0.001	− 0.018127	0.458	0.5881

Table 1. Peak differentiation associations with age peak differentiation is significantly associated with increased age in whole brain, and regional calculations. Biological sex is included as a covariate and was found to not be associated with peak differentiation. Effect age describes association of peak differentiation with one year increase in chronological age.

with areas of hypoperfusion[29] and microstructural changes on imaging[30]. T1-weighted hypointensities have also been shown to co-vary with multiple sclerosis disease progression[31]. These findings support the interpretation that diminished GM–WM differentiation reflects microstructural compromise. While the specific biological mechanisms underlying this peak measure remain unclear, potential contributors may include white matter demyelination, gray matter dendritic pruning, or inflammation. However, our metric does not directly differentiate among these possibilities, and further studies would be needed to clarify the underlying mechanisms.

The whole-brain peak differentiation is distinct from GM/WM contrast, which also declines with age[9,20,25,27,32–34]. The whole-brain peak differentiation measure we report, however, does not require that voxel

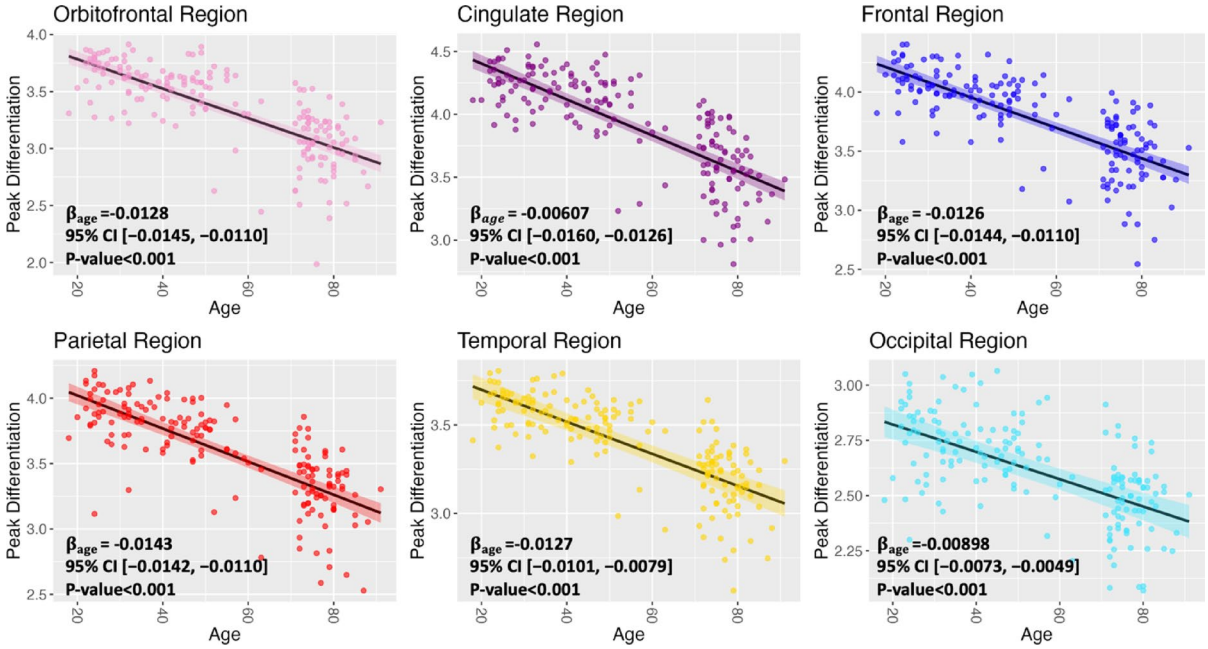

Fig. 4. Regional Peak Differentiation associations with age ($n = 178$). Peak differentiation is plotted on y-axis. Chronological age is plotted on the x-axis. Lower peak differentiation is associated with higher age in each lobar region.

intensities be sampled at a specified distance from the GWI, as in methods previously reported to quantify GM/WM contrast[9,20,25]. Additionally, GM/WM contrast is essentially a mean intensity comparison, with no consideration of the distribution of voxel intensities. In contrast, whole-brain peak differentiation provides a summary metric derived from all brain voxel intensities, including deep and superficial WM and GM. By assessing the intensity distribution across all voxels, it offers a more robust, comprehensive reflection of global tissue differences, especially in regions where surface reconstruction is challenging. For example, when image intensities are nearly homogeneous within gray and white matter respectively, the value of the proposed peak differentiation will be very high because of small denominator in Eq. 1. When image intensities within tissues are heterogeneous, the denominator grows while the numerator remains as before reducing the value of peak differentiation. On the other hand, previously suggested methods to quantify GM/WM contrast[9,20,25] will produce nearly identical values in both of these scenarios because they are essentially a mean intensity comparison.

Peak differentiation is also distinct from WM volume[21], GM volume[22], and cortical thickness[23], which only account for anatomical size without deriving information from voxel intensities. In contrast, whole-brain peak differentiation provides a summary metric derived from all brain voxel intensities, including deep and superficial WM and GM. By assessing the intensity distribution across all voxels, it offers a robust, comprehensive reflection of global tissue differences, especially in regions where surface reconstruction is challenging. This quantitative approach can characterize GWI effects that are not necessarily visible on inspection of images (Fig. 2). Our whole brain peak-differentiation metric is fully automated, does not require tissue segmentation or lesion masking, and includes normalization by standard deviation which carries information about tissue heterogeneity. These features make the method sensitive, computationally efficient, and potentially easier to implement across diverse clinical workflows. Rather than focusing on a disease-specific cohort, we provide a proof-of-concept in a large healthy sample, emphasizing the metric's potential applicability to a range of future studies.

Our histogram-based contrast approach shares conceptual similarity with that of De Guio et al. (2014), who examined intensity distributions in the context of CADASIL[35]. However, their method included lesion masking and pathology-specific segmentation steps, which were not used in our healthy aging cohort. Additionally, their contrast metric was not normalized by standard deviation, and therefore did not take tissue heterogeneity into account. Moreover, their analysis did not explicitly characterize age-related effects. Our study builds on these ideas by offering a more generalizable methodology, requiring minimal segmentation and registration, for exploring gray-white matter contrast in normative populations.

Overall, this metric may complement established biomarkers such as cortical thickness, regional volume and GM/WM contrast by providing a global, voxel-based measure of tissue differentiation, which accounts for tissue heterogeneity and requires minimal segmentation, thereby offering an alternative lens on structural brain differentiation.

Limitations

Our study did not include extensive validation using repeated scans on multiple scanners, which would be a valuable next step. The small, two-participant, stability study we included nevertheless demonstrates the peak differentiation is not driven by SNR considerations, thereby showing its robustness.

Voxel intensity on T1W images is on an arbitrary scale determined by tissue properties such as T1 of the tissue and several instrumental factors such as flip angle, receive coil profile, bandwidth, partial Fourier factor and voxel size. Therefore, image intensities are first linearly scaled to be 0-3000. Furthermore, peak differentiation is scale free because it is defined as a ratio of difference in image intensities to their standard deviation. Non-instrumental factors such as changes in tissue T1 or proton density are those that drive the peak differentiation sensitivity to aging.

An additional limitation is the use of a Gaussian mixture model with constrained equal variances to define peak differentiation. This assumption was adopted to stabilize fitting and enforce a standardized, scale-free metric across participants, although it may not perfectly capture asymmetries in the true tissue intensity distributions. As seen in Fig. 2, minor deviations between the fitted mixture and the empirical histogram suggest mild model misalignment. Accordingly, peak differentiation should be interpreted as a global index of GM–WM separation rather than a precise biophysical estimator of tissue class. Nevertheless, the robust and regionally consistent age associations observed across the cortex indicate that the primary biological inferences are unlikely to be driven by this modeling constraint.

Besides carrying biological information, voxel intensity in T1W images is also sensitive to positioning of the head in the radiofrequency coil. Spatial variation of coil sensitivity across the brain may partially obscure the peaks in the histogram. Despite addressing this issue on two levels -- a correction during image reconstruction on the scanner and post-acquisition preprocessing using FSL's FAST - the residual uncorrected variation may have remained in part and could be more prominent if a surface coil were used. Additionally, our finding that peak differentiations derived from cerebral GWI subregions recapitulate whole-brain findings makes a regional bias unlikely. Bias fields effects would also not explain the robust age associations characterized in this study which largely remain the same in the absence of the corrections (Supplemental Table 5). Small susceptibility correction in T1W images is a standard step in our processing pipelines but for the purposes of this analysis likely has negligible effect and could be skipped.

Peak differentiation is minimally sensitive to noise. In our preliminary verification, the ratio of low noise whole-brain peak differentiation to high noise peak differentiation was only 1.01 and 1.004. If noise had a strong influence, this ratio would be around 2.45. This confirms that peak differentiation is minimally sensitive to noise and is a valid measure of GM and WM distribution, distinct from GM/WM contrast, which relies on sampled mean intensity ratios.

Peak differentiation is not sensitive to the overall scaled T1W image intensity because we intentionally defined the measure as a ratio scaled to the standard deviation. Furthermore, to characterize the role of standard deviation in the association of peak differentiation and age, we tested for association of standard deviation with age. Standard deviation is shown to be differentially associated with age in different regions (Supplemental Table 1), in comparison to peak differentiation which declines with age in all regions. This suggests that associations of peak differentiation with age are driven by GM-WM distributions, and that incorporating standard deviation is necessary to account for regional signal variations. Furthermore, standard deviation associations with age may partially describe age-related changes in tissue heterogeneity and density (Supplemental Table 1). However, $\mu 2 - \mu 1$ is also shown to be associated with age (Supplemental Table 2). These associations are then incorporated into the scale-free peak differentiation measure.

Future directions

Subject to further confirmation and validation in aging and in brain diseases, the whole-brain peak differentiation approach could potentially serve as a quantitative metric of brain age, to detect subtle changes like accelerated aging or pathology that might otherwise go unnoticed. Future studies can probe how deviations from age-appropriate peak differentiation norms may indicate abnormal aging or diffuse brain pathology, even in the absence of visible abnormalities. Regional peak differentiation from juxtacortical regions could also enhance sensitivity to pathology affecting the GWI, such as neurodegenerative disease and trauma. Subsequent studies could explore peak differentiation as an imaging marker for neurodegenerative diseases, building upon prior research that links a lower GM/WM intensity ratio to individuals with mild cognitive impairment who progress to dementia on 3-year follow up[36]. While further validation is needed, combining peak differentiation with measures such as GM/WM intensity ratio, cortical thickness and amyloid PET could be explored to enhance prediction of Alzheimer's Disease status and prognosis[37]. It is not our intent to replace GM/WM contrast but to instead offer an additional measure for GM-WM distribution that can readily be implemented in clinic.

Conclusion

In conclusion, we demonstrate feasibility of an automated whole brain peak differentiation measurement to characterize brain aging in a healthy cohort, with minimal reliance on segmentation or other processing. Future implementation for routine assessment of standard clinical T1W images could serve as a screening approach feasible to implement in a clinical setting.

Data availability

Data and code will be made available upon request from the corresponding author M.L.L.

Received: 13 February 2025; Accepted: 28 December 2025
Published online: 13 January 2026

References

1. Alisafaei, F. et al. Mechanisms of local stress amplification in axons near the gray-white matter interface. *Biophys. J.* **119**(7), 1290–1300 (2020).
2. Cullen, D. K. et al. A porcine model of traumatic brain injury via head rotational acceleration. *Methods Mol. Biol.* **1462**, 289–324 (2016).
3. Thatcher, R. W. et al. Quantitative MRI of the gray-white matter distribution in traumatic brain injury. *J. Neurotrauma*. **14**(1), 1–14 (1997).
4. Blackmon, K. et al. Cortical gray-white matter blurring and cognitive morbidity in focal cortical dysplasia. *Cereb. Cortex*. **25**(9), 2854–2862 (2015).
5. Wu, S. et al. Nervous system injury and neuroimaging of zika virus infection. *Front. Neurol.* **9**, 227 (2018).
6. Mahajan, K. R. et al. Juxtacortical susceptibility changes in progressive multifocal leukoencephalopathy at the gray-white matter junction correlates with iron-enriched macrophages. *Mult Scler.* **27**(14), 2159–2169 (2021).
7. Nasiri, E. et al. Radiological features of late-onset multiple sclerosis: A systematic review and meta-analysis. *J. Neuroradiol.* **50**(6), 571–580 (2023).
8. Phillips, O. R. et al. The superficial white matter in Alzheimer's disease. *Hum. Brain Mapp.* **37**(4), 1321–1334 (2016).
9. Salat, D. H. et al. Age-associated alterations in cortical gray and white matter signal intensity and gray to white matter contrast. *Neuroimage* **48**(1), 21–28 (2009).
10. Katz, M. J. et al. Age-specific and sex-specific prevalence and incidence of mild cognitive impairment, dementia, and Alzheimer dementia in Blacks and whites: a report from the Einstein Aging Study. *Alzheimer Dis. Assoc. Disord.* **26**(4), 335–343 (2012).
11. Fleysher, R. et al. White matter structural integrity and transcranial Doppler blood flow pulsatility in normal aging. *Magn. Reson. Imaging*. **47**, 97–102 (2018).
12. Cusack, R., Brett, M. & Osswald, K. An evaluation of the use of magnetic field maps to undistort echo-planar images. *Neuroimage* **18**(1), 127–142 (2003).
13. Jezzard, P. & Balaban, R. S. Correction for geometric distortion in echo planar images from B0 field variations. *Magn. Reson. Med.* **34**(1), 65–73 (1995).
14. Hoopes, A. et al. SynthStrip: skull-stripping for any brain image. *NeuroImage* **260**, 119474 (2022).
15. Guillemaud, R. & Brady, M. Estimating the bias field of MR images. *IEEE Trans. Med. Imaging.* **16**(3), 238–251 (1997).
16. Zhang, Y., Brady, M. & Smith, S. Segmentation of brain MR images through a hidden Markov random field model and the expectation-maximization algorithm. *IEEE Trans. Med. Imaging.* **20**(1), 45–57 (2001).
17. Gudbjartsson, H. & Patz, S. The Rician distribution of noisy MRI data. *Magn. Reson. Med.* **34**(6), 910–914 (1995).
18. Scrucca, L. F., Murphy, C., Brendan, T. & Raftery, A. E. *Model-Based Clustering, Classification, and Density Estimation Using {mclust} in {R}*. (Chapman and Hall/CRC, 2023).
19. Team, R. C. *R: A Language and Environment for Statistical Computing*. https://www.R-project.org/ (2022).
20. Fischl, B. FreeSurfer. *Neuroimage.* **62**(2), 774–781 (2012).
21. Fujita, S. et al. Characterization of brain volume changes in aging individuals with normal cognition using serial magnetic resonance imaging. *JAMA Netw. Open.* **6**(6), e2318153 (2023).
22. Hedman, A. M. et al. Human brain changes across the life span: a review of 56 longitudinal magnetic resonance imaging studies. *Hum. Brain Mapp.* **33**(8), 1987–2002 (2012).
23. Fjell, A. M. et al. High consistency of regional cortical thinning in aging across multiple samples. *Cereb. Cortex*. **19**(9), 2001–2012 (2009).
24. Magnaldi, S. et al. Contrast between white and grey matter: MRI appearance with ageing. *Eur. Radiol.* **3**(6), 513–519 (1993).
25. Westlye, L. T. et al. Increased sensitivity to effects of normal aging and Alzheimer's disease on cortical thickness by adjustment for local variability in gray/white contrast: a multi-sample MRI study. *Neuroimage* **47**(4), 1545–1557 (2009).
26. Davatzikos, C. & Resnick, S. M. Degenerative age changes in white matter connectivity visualized in vivo using magnetic resonance imaging. *Cereb. Cortex*. **12**(7), 767–771 (2002).
27. Raz, N., Millman, D. & Sarpel, G. Cerebral correlates of cognitive aging: gray-white-matter differentiation in the medial temporal lobes, and fluid versus crystallized abilities. *Psychobiology* **18**(4), 475–481 (1990).
28. van Walderveen, M. A. et al. Histopathologic correlate of hypointense lesions on T1-weighted spin-echo MRI in multiple sclerosis. *Neurology* **50**(5), 1282–1288 (1998).
29. Narayana, P. A. et al. Hypoperfusion and T1-hypointense lesions in white matter in multiple sclerosis. *Mult Scler.* **20**(3), 365–373 (2014).
30. Lapucci, C. et al. Degree of microstructural changes within T1-SE versus T1-GE hypointense lesions in multiple sclerosis: relevance for the definition of black holes. *Eur. Radiol.* **30**(7), 3843–3851 (2020).
31. Truyen, L. et al. Accumulation of hypointense lesions (black holes) on T1 spin-echo MRI correlates with disease progression in multiple sclerosis. *Neurology* **47**(6), 1469–1476 (1996).
32. Grydeland, H. et al. Improved prediction of Alzheimer's disease with longitudinal white matter/gray matter contrast changes. *Hum. Brain Mapp.* **34**(11), 2775–2785 (2013).
33. Vidal-Piñeiro, D. et al. Accelerated longitudinal gray/white matter contrast decline in aging in lightly myelinated cortical regions. *Hum. Brain Mapp.* **37**(10), 3669–3684 (2016).
34. Lewis, J. D. et al. Cortical and subcortical T1 white/gray contrast, chronological age, and cognitive performance. *NeuroImage* **196**, 276–288 (2019).
35. De Guio, F. et al. Decreased T1 contrast between gray matter and normal-appearing white matter in CADASIL. *AJNR Am. J. Neuroradiol.* **35**(1), 72–76 (2014).
36. Jefferson, A. L. et al. Gray & white matter tissue contrast differentiates mild cognitive impairment converters from non-converters. *Brain Imaging Behav.* **9**(2), 141–148 (2015).
37. Putcha, D. et al. Gray to white matter signal ratio as a novel biomarker of neurodegeneration in Alzheimer's disease. *Neuroimage Clin.* **37**, 103303 (2023).

Author contributions

Joan Y. Song: ** Conceptualization, Methodology, Investigation, Formal analysis, Visualization, Writing-original draft, Writing-review and editing. **Roman Fleysher: ** Methodology, Formal analysis, Data, Supervision, Writing-review and editing. **Kenny Ye: ** Methodology, Formal analysis, Writing-original draft, Writing-review and editing. **Jenasis Ortega: ** Data curation and validation. **Mimi Kim: ** Methodology, Formal analysis, Writing-original draft, Writing-review and editing. **Molly E Zimmerman : Supervision, Writing-review and editing. **Richard B Lipton** , Methodology, Investigation, Formal analysis, Supervision, Writing-original draft, Writing-review and editing. **Michael L. Lipton** , Conceptualization, Methodology, Investigation, Formal analysis, Supervision, Writing-original draft, Writing-review and editing.

Funding
This project was supported in part by a grant [2P01AG003949] from the National Institute on Aging to RBL. Trainee support to JYS from the Medical Scientist Training Program (T32GM149364).

Declarations

Ethics approval
This study was reviewed and approved by the Albert Einstein College of Medicine IRB on 11/16/2023 (IRB # 2021–13702). All participants provided written informed consent.

Competing interests
The authors declare no competing interests.

Additional information
Supplementary Information The online version contains supplementary material available at https://doi.org/10.1038/s41598-025-34355-y.

Correspondence and requests for materials should be addressed to M.L.L.

Reprints and permissions information is available at www.nature.com/reprints.

Publisher's note Springer Nature remains neutral with regard to jurisdictional claims in published maps and institutional affiliations.